Proceedings of ASME Turbo Expo 2011
GT2011
June 6-10, 2011, Vancouver, British Columbia, Canada

GT2011-46106

COMBINED EFFECTS OF WAKES AND PULSED VORTEX GENERATOR JET FLOW CONTROL ON BOUNDARY LAYER SEPARATION ON A VERY HIGH LIFT LOW PRESSURE TURBINE AIRFOIL

Ralph J. Volino
Mechanical Engineering Department
United States Naval Academy
Annapolis, Maryland 21402-5042
volino@usna.edu

ABSTRACT

Boundary layer separation control with pulsed vortex generator jets (VGJs) has been studied on a very high lift, low-pressure turbine airfoil in the presence of unsteady wakes. Experiments were done under low (0.6%) and high (4%) freestream turbulence conditions on a linear cascade in a low speed wind tunnel. Cases were considered at Reynolds numbers (based on the suction surface length and the nominal exit velocity from the cascade) of 25,000 and 50,000. Wakes were produced from moving rods upstream of the cascade with flow coefficient 1.13 and rod spacing equal 2 blade pitches, resulting in a dimensionless wake passing frequency $F=fL_{j-te}/U_{ave}=0.14$, where f is the frequency, L_{j-te} is the length of the adverse pressure gradient region on the suction surface, and U_{ave} is the average freestream velocity. The VGJs were injected at the beginning of the adverse pressure gradient region on the suction surface with maximum jet velocity in each pulse equal to the local freestream velocity and a jet duty cycle of 10%. Several different timings of the VGJs with respect to the wakes were considered. Pressure surveys on the airfoil surface and downstream total pressure loss surveys were documented. Instantaneous velocity profile measurements were acquired in the suction surface boundary layer and downstream of the cascade. In cases without VGJs, the boundary layer momentarily reattached in response to the wake passing, but separated between wakes. The VGJs also caused reattachment, and if the VGJ pulsing frequency was sufficiently high, separation was largely suppressed for the full wake passing cycle. The timing of the VGJs with respect to the wakes was not very important. The jet pulsing frequency needed for separation control was about the same as found previously in cases without wakes. The background freestream turbulence effect was negligible in the presence of the larger wake and VGJ disturbances.

NOMENCLATURE

Cp	$2(P_T-P)/(\rho U_e^2)$, pressure coefficient
C_x	axial chord length
F	fL_{j-te}/U_{ave}, dimensionless frequency
f	wake passing frequency
L_{j-te}	length of adverse pressure gradient region on suction surface
L_s	suction surface length
L_ϕ	blade spacing (pitch)
P	pressure
P_S	upstream static pressure
P_T	upstream stagnation pressure
P_{Te}	downstream stagnation pressure
Re	U_eL_s/ν, exit Reynolds number
s	streamwise coordinate, distance from leading edge
T	period of jet pulsing cycle
t	time
TI	background freestream turbulence intensity
U	local mean velocity
U_{ave}	average freestream velocity in adverse pressure gradient region
U_i	inlet freestream velocity
U_e	nominal exit freestream velocity, based on inviscid solution
U_{rod}	wake generator velocity
u'	rms fluctuating streamwise velocity
x	axial distance from leading edge
α_i	inlet flow angle
ϕ	coordinate along blade spacing, normal to axial chord
ν	kinematic viscosity
ρ	density
ψ	$(P_T-P_{Te})/(P_T-P_S)$, total pressure loss coefficient
ζ	$U_i\cos(\alpha_i)/U_{rod} = U_{axial}/U_{rod}$, flow coefficient

INTRODUCTION

Boundary layer separation on the suction side of low-pressure turbine (LPT) airfoils can cause partial loss of lift and high aerodynamic losses (Hourmouziadis [1], Mayle [2], Sharma et al. [3]). In aircraft engines the lower Reynolds numbers at altitude can lead to a component efficiency drop of 2% between takeoff and cruise in large commercial transport engines, and possibly as much as 7% in smaller engines operating at higher altitudes [4, 5]. Separation becomes more likely when airfoil loading is high because of the strong adverse pressure gradients on the suction surface, but high loading is desirable since it can be used to reduce airfoil count, weight and cost. Accurate prediction of separation under relevant conditions, including the effects of boundary layer transition and periodic unsteadiness, is needed to design high lift airfoils without separation problems.

Separation can be mitigated in a few ways. One is by wakes shed from the airfoils in upstream stages in an engine. The velocity deficit and elevated turbulence in periodic wakes help to suppress separation and can cause a separated boundary layer to reattach. Hodson and Howell [6] describe the mechanisms by which wakes promote reattachment, including the "negative jet" which results when the velocity deficit in the wake causes the flow outside the wake to accelerate and impinge on the surface, and the unsteadiness which promotes transition in the boundary layer. Following the wake itself is a calmed period (Gostelow et al. [7] and Schulte and Hodson [8]) in which the boundary layer has low turbulence and greater resistance to separation. Numerous studies have considered the wake effect in the LPT, including those listed in Hodson and Howell [6], and more recent references in Bons et al. [9] and Pluim et al. [10]. Examples include Schobeiri et al. [11], Öztürk and Schobeiri [12], Jiang and Simon [13], and Mahallati and Sjolander [14] who all used the Pack B airfoil. Zhang and Hodson [15] and Funazaki et al. [16] used more highly loaded airfoils. Many additional studies are available from these research groups and others.

Separation problems can also be limited through good airfoil design, as described by Praisner and Clark [17]. In recent years, knowledge of wake effects has allowed for designs with higher loading than would be possible under steady inflow conditions. Even with the best design methods, however, a loading limit will always exist, above which separation will still occur. Flow control, either active or passive, might allow an extension of this limit.

Separation control with passive devices such as boundary layer trips has been shown effective by Zhang et al. [18], Bohl and Volino [19], Volino [20], and others. Passive devices have the distinct advantage of simplicity, but they also introduce parasitic losses and cannot be adjusted to account for changes in flow conditions. Active devices are also possible, and although their complexity and reliability would create challenges, they could be made adjustable and provide potentially better control. In turbomachinery, plasma devices as used by Huang et al. [21] could be viable, and are under active study. Vortex generator jets (VGJs), as introduced by Johnston and Nishi [22], have also been considered. Blowing from small, compound angled holes is used to create streamwise vortices which promote transition and bring high momentum fluid into the near wall region to help control separation. The most effective VGJs enter the boundary layer at a relatively shallow pitch angle (typically 30 to 45 degrees) relative to the wall and a high skew angle (45 to 90 degrees) relative to the main flow. Bons et al. [4, 23], Volino [24], Volino and Bohl [25], McQuilling and Jacob [26], and Eldredge and Bons [27] all used VGJs on the highly loaded Pack B LPT airfoil. Separation was essentially eliminated, even at the lowest Reynolds number considered. Similar results with were found on the very highly loaded L1M airfoil by Bons et al. [28], who saw the size of a large separation bubble reduced by VGJs. Pulsed jets were more effective than steady jets in all studies. The initial disturbance created by each pulse caused the boundary layer to attach. The boundary then remained resistant to separation during the calmed period which followed the VGJ disturbance. When the time between pulses was long enough, the boundary layer did eventually relax to a separated state, but due to the control which persisted during the calmed period, the VGJs were effective even with low jet pulsing frequencies, duty cycles and mass flow rates. Since the boundary layer was attached and undisturbed for much of the jet pulsing cycle, profile losses were low.

The present study uses the L1A airfoil, which was designed at the Air Force Research Laboratory (AFRL) and is available on a limited basis from Clark [29]. Dimensions of the L1A as used in the present study are given in Table 1. It was deliberately designed to provide a challenging case for flow control. The L1A has a Zweifel coefficient of 1.35, which corresponds to 10% higher loading than the "ultra-high lift" airfoils described by Zhang and Hodson [30], and 17% higher loading than the Pack B airfoil. The L1A is also aft loaded, which is advantageous for reducing secondary flow losses at the endwalls, but makes the boundary layer more prone to separation than a forward loaded blade, as documented in Bons et al. [9], Volino [31], Ibrahim et al. [32], and Volino et al. [33]. In cases without wakes and low Reynolds numbers, the boundary layer separates and does not reattach, in spite of transition to turbulence in the shear layer over the separation bubble. This result contrasts with the results of studies on less aggressive airfoils (e.g. Volino [34]), which all showed reattachment after transition. The failure to reattach can occur even when transition starts farther upstream on the L1A than on other airfoils (e.g. with low freestream turbulence and Re=100,000, transition starts at s/L_s=0.8 on the Pack B and causes reattachment, and at s/L_s=0.6 on the L1A without reattachment). The adverse pressure gradient on the L1A is roughly twice as strong as on the Pack B, and is apparently strong enough to prevent reattachment at low Reynolds numbers in spite of transition and turbulent mixing in the shear layer over the separation bubble. The failure of the boundary layer to reattach results in a 20% loss in lift and increases profile losses by up to a factor of 7. At higher Reynolds numbers the separation bubble closes, and for $Re\geq$200,000 the separation bubble on the L1A is small and the boundary layer is attached over most of the airfoil.

Two studies have considered the effect of wakes on the L1A boundary layer. Bons et al. [9] considered a case with Re=50,000 (based on the suction surface length and the nominal exit velocity from the cascade), background freestream turbulence TI=3%, and periodic wakes produced with moving rods upstream of the airfoils. The dimensionless frequency of the wake passing was $F=fL_{j\text{-}te}/U_{ave}$=0.34, where $L_{j\text{-}te}$ is the length of the adverse pressure gradient region on the suction surface, and U_{ave} is the average freestream velocity over this distance. The length $L_{j\text{-}te}$ is also the distance from a row of vortex generator jet (VGJ) holes to the trailing edge. Volino [35] considered cases at high (4%) and low (0.6%) freestream turbulence with Re=25,000 and 50,000. The spacing and speed of moving rods were varied to produce wake passing frequencies between F=0.14 and 0.56. Wakes largely suppressed separation at Re=25,000 when F was above 0.5. At lower frequencies the disturbances caused by the wakes caused momentary reattachment, but the boundary layer re-separated between wake passing events. For Re=50,000, F=0.3 was sufficient to largely suppress separation. The effect was the same whether a particular frequency was achieved by changing rod spacing or rod velocity. Higher freestream turbulence helped to promote transition and reattachment, but the effect was small compared to the wake passing effect.

Flow control with vortex generator jets on the L1A has been considered in Bons et al. [9], Volino et al. [36, 37, 38], and Ibrahim et al. [39, 40]. The same Reynolds numbers and freestream turbulence levels were considered as with the wakes. With a VGJ blowing ratio of 1 (i.e. maximum jet velocity equal to the freestream velocity) and 10% duty cycle, a dimensionless jet pulsing frequency of F=0.5 was sufficient to control separation with Re=25,000, and F=0.3 was sufficient for Re=50,000. These frequencies match the wake passing frequencies required for separation control at each Reynolds number, suggesting that the type of disturbance is not as important as the frequency of the disturbance for controlling the boundary layer. At lower frequencies the flow control was not as good, and the boundary layer separated between pulses.

The combined effect of wakes and vortex generator jets on separation control has been studied on the Pack B airfoil by Bloxham et al. [41] and on the L1A by Bons et al. [9]. On the L1A, a case was considered with Re=50,000, 3% freestream turbulence, and dimensionless wake passing frequency F=0.34. The VGJ pulsing frequency was equal to the wake passing frequency, and the timing of the jets was varied relative to the wakes. Without VGJs the wakes caused only partial separation control. With the VGJs injected near the pressure minimum on the suction side, good separation control was achieved even without wakes. The timing of the jets to the wakes was, therefore, unimportant. When the VGJs were injected farther downstream, they were only effective when combined with wakes and the effectiveness depended on the timing.

In the present study, the combined effect of wakes and VGJs is considered with Re=25,000 and 50,000 under low (0.6%) and high (4%) freestream turbulence conditions. These Reynolds numbers are very low, but could still be of interest in small engines operating at high altitudes (e.g. in future unmanned vehicles). They are also of interest for the present study because they result in a very large separation bubble, providing a challenging case for flow control and a good case for exploring the response of the boundary layer to VGJs and wakes. The wake passing frequency is set to a low value so that without flow control the boundary layer only intermittently reattaches during wake passing events. Cases with various VGJ frequencies and timings relative to the wake passing are documented. Surface pressure distributions, total pressure loss profiles, and instantaneous boundary layer velocity measurements are used to show how wakes and VGJs combine to affect separation.

EXPERIMENTAL FACILITY AND MEASUREMENTS

Experiments were conducted in a closed loop wind tunnel with a seven blade linear cascade as shown in Fig. 1. A fine screen located upstream of the cascade is used to break up the boundary layers which form upstream of the test section and to provide uniform inlet conditions to the cascade. The freestream turbulence entering the cascade was measured with a cross-wire probe positioned just upstream of the center blade. The turbulence intensity is 0.8% in the streamwise component and 0.5% in the cross stream components. The integral length scale of the streamwise component is $0.47C_x$. To produce high freestream turbulence, the screen is replaced with a coarse grid, consisting of a 1.5 mm thick sheet metal plate with 19 mm square holes spaced 25.4 mm apart, center to center, in both directions. In a plane perpendicular to the inlet flow and $1.7C_x$ upstream of the center blade, the grid produced uniform flow with TI=6.0% in the streamwise component and 4.2% in the cross stream components, for an overall intensity of 4.9%. The streamwise component was also measured at the inlet plane of the cascade in the four center passages, where it had decayed to about 4.2%. Downstream of the cascade, the local TI is 1.8% across all passages. The local freestream turbulence intensity in the passage at the beginning of the adverse pressure gradient region is 1.4%. The change in TI through the passage is due mainly to the change in the local freestream velocity along with some decay of the turbulence. The upstream integral length scale of the freestream turbulence is $0.12C_x$ in the streamwise component and $0.04C_x$ in the other components. Further details of the facility and inlet flow are in Volino et al. [33].

A tailboard and two flaps, shown in Fig. 1, are needed to produce the correct inlet and exit flow angle from the cascade. Their position was set to produce periodicity at high Reynolds numbers as discussed in Volino [35]. At low Reynolds numbers, when significant separation bubbles are present, the periodicity is not as good due to suppression of the separation bubble thickness on the blades closest to the tailboard. In cases where wakes or other flow control suppress separation, periodicity is reestablished. The lack of periodicity in

Table 1: Cascade parameters

Axial Chord, C_x [mm]	True Chord [mm]	Pitch, L_ϕ [mm]	Span [mm]	Suction side, L_s [mm]	Inlet flow angle	Exit flow angle
134	146	136	724	203	35°	60°

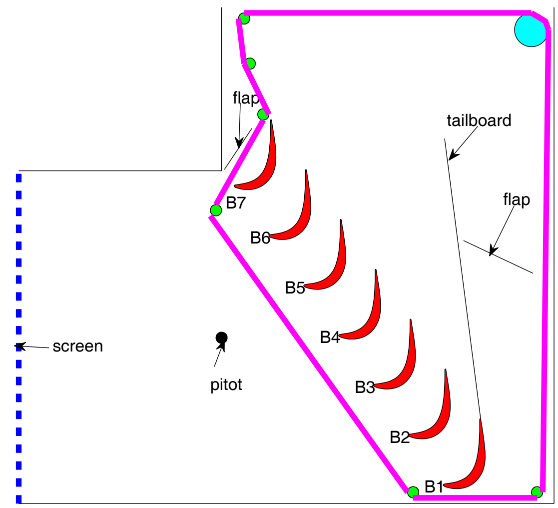

Fig. 1 Schematic of linear cascade with wake generator

cases with large separation bubbles is considered acceptable since the focus of the research is separation control, and not documentation of cases with large separation that would be unacceptable in practice. This compromise facilitates the study of a larger number of cases by obviating the need to adjust the tailboard by trial and error for each case. It also provides for better repeatability in the experiments, since the position of the tailboard is fixed for all cases. Any changes in separation with wakes or VGJs will be larger in practice than documented in the experiment, due to the effect of the tailboard in suppressing the bubble size in the uncontrolled cases.

The wake generator includes a chain near each endwall of the cascade that passes $0.54C_x$ upstream of the leading edges of the cascade blades. The chains then pass downstream around blade B7 on the inside turn of the cascade and pass well downstream of the cascade before returning upstream around blade B1 on the outside turn of the cascade. This completes the chain circuit. The magenta line surrounding the cascade in Fig. 1 shows the location of the chain. A traverse for probe movement is located within the chain circuit downstream of the blade row. Each chain is driven by a drive gear (large circle in Fig. 1) and also passes around six idler sprockets (small circles). One of the idler sprockets is adjustable to maintain tension in the chain. The drive gears for the upper and lower chains are on a common axle and driven by a single electric motor so both chains move in unison. The motor speed is set with a variable frequency inverter. The chain links have hollow pins, through which the wake generator rods are attached. Each rod consists of a 4 mm diameter carbon fiber tube with a steel pin attached at each end. The steel pins are inserted through the holes in the upper and lower chain, and then secured with small clips. The distance between rods was 272 mm, which correspond to $2L_\phi$, where L_ϕ is the blade spacing in the cascade. The ratio of rod to blade spacing is at the very high end of what might be found for vane to rotor blade spacing in an engine. The ratio of vane to rotor blade spacing is typically about 1.6 as indicated by Bloxham et al. [41], so the high ratio in the present case provides a more challenging case for flow control, as shown in Volino [35].

The ratio of the rod diameter to the axial chord is 0.03, which is consistent with the wake generators of Bons et al. [9] and Funazaki et al. [16]. The rods are smaller than those of Kaszeta et al. [42] who had a diameter to chord ratio of 0.06. The present rods are larger than those of Schobeiri et al. [11] and Zhang and Hodson [15] who had rod diameter to chord ratios of about 0.01. In the present study, as in Bons et al. [9] and Kaszeta et al. [42], the rod wakes are intended to simulate the wakes of very highly loaded airfoils under low Reynolds number conditions with thick boundary layers and in some cases large separation bubbles. A large diameter rod is therefore needed to simulate an airfoil wake with a large velocity deficit. The velocity deficit and turbulence level in the rod wakes are documented in Volino [35], and compared to the wakes of the cascade airfoil. The rod wakes were found to be reasonable approximations of airfoil wakes. At the cascade inlet, the peak turbulence level in the rod wakes was 14%, and the level between wakes was at the background *TI* in the wind tunnel.

The rods were driven at a velocity of 0.73 times the cascade inlet velocity, U_i. This gives a flow coefficient, $\zeta = U_i\cos(\alpha_i)/U_{rod}$=1.13, where α_i is the inlet flow angle. This is at the high end of the expected range for an engine. The flow coefficient and rod spacing were chosen to be large to provide cases in which the wakes alone would not completely eliminate separation. This allows for investigation of the interaction of the wakes and VGJs in controlling separation. The dimensionless wake passing frequency is F=0.14. The timing of the wake generator is recorded with an infrared photo detector, which senses the passage of each rod and emits a voltage that is used to trigger a function generator which drives the solenoid valves used to produce the pulsed VGJs. The signal to the valves is recorded with other data, allowing phase averaging of the results.

To produce the VGJs, each blade in the cascade has a central cavity which extends along the entire span. As explained in Volino et al. [36], compressed air is supplied to the cavities from a common manifold. The manifold is supplied through two fast response solenoid valves (Parker Hannifin 009-0339-900 with General Valve Iota One pulse driver) operating in parallel. A single spanwise row of holes was drilled into the suction surface of each blade at the inviscid pressure minimum location, s/L_s=0.5 (x/C_x=0.62), where s is the distance from the leading edge and L_s is the suction surface length. The pressure minimum has been shown in the studies listed above to be about the optimal location for flow control devices. The holes are 0.8 mm (0.006C_x) in diameter and drilled at 30° to the surface and 90° to the main flow direction. This is the same orientation used in all the VGJ studies listed above. The hole spacing is 10.6 diameters, and the length to diameter ratio is 12. When the solenoid valves are opened, the jet velocity rises quickly for about 0.01 s to a maximum and then immediately begins to drop. If the period of the pulse is long enough the velocity reaches a steady value, but for the short duration pulses of the present study, the 0.01 s rise time compares to valve-open times between about 0.01 s and 0.03 s, so there is insufficient time for the jet velocity to reach a steady value. When the valves close, the jet velocity quickly drops to zero. The maximum jet velocity in each pulse is used to define the blowing ratio and is set equal to the nominal local freestream velocity at the VGJ holes, for a blowing ratio of 1. The jet duty cycle is 10%. The mass flow rate of the jets is approximately 0.004% of the main flow mass flow rate. More on the characteristics of the pulses is available in Volino et al. [36].

Nine different VGJ timings relative to the wakes were considered, as shown in Fig. 2. Timings were chosen to place the jet pulses at different times within or between wakes. Case (a) is the baseline case with only wakes. Cases (b-d) have a single pulse for each wake passing. Timings (e-g) have two pulsed per wake period. To maintain

Table 2: Velocity profile measurement stations

Station	1	2	3	4	5	6
s/L_s	0.53	0.59	0.69	0.78	0.88	0.97
x/C_x	0.65	0.72	0.80	0.86	0.92	0.97

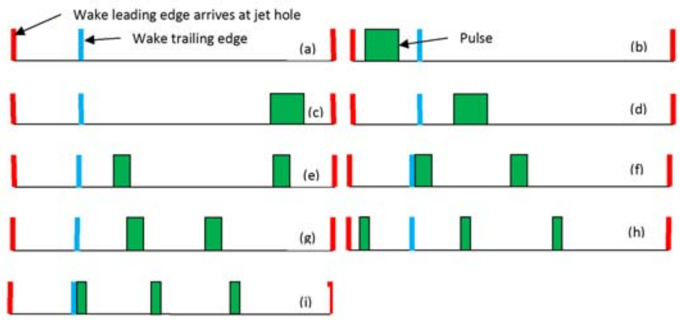

Fig. 2 VGJ timings (a) through (i)

the same overall blowing period, the pulses in cases (e-g) are half as long as those in (b-d). Timings (h-i) have three pulses per wake.

Measurements

The center blade, designated B4 in Fig. 1, contains pressure taps near the spanwise centerline. Pressure surveys are made using a pressure transducer (0-870 Pa range Validyne transducer). Stagnation pressure is measured with a pitot tube upstream of the cascade and wake generator. The uncertainty in the suction side pressure coefficients, Cp, is 0.07. Most of this uncertainty is due to bias error. Stochastic error is minimized by averaging pressure transducer readings acquired at a 10 kHz sampling rate over a 10 second period.

Total pressure losses are documented using a Kiel probe traversed across three blade spacings, 0.63C_x downstream of the cascade. A traverse is located in the wind tunnel downstream of the cascade to move the probe. The traverse causes an acceptably low blockage when it is located at least two C_x downstream of the cascade.

Velocity profiles on the suction surface were measured at the six streamwise stations listed in Table 2. All stations are downstream of the inviscid pressure minimum at s/L_s=0.49. Profiles were acquired near the spanwise centerline of the airfoil with a hot-wire anemometer (AA Lab Systems model AN-1003) and a single sensor hot-film probe (TSI model 1201-20). The sensor diameter is 51 μm, and the active length is 1.02 mm. At each measurement location, data were acquired for 26 seconds at a 20 kHz sampling rate (2^{19} samples). All raw data were saved. The high sampling rate provides an essentially continuous signal, and the long sampling time results in low uncertainty in both statistical and spectral quantities. Data were acquired at 40 wall normal locations in each profile, extending from the wall to the free-stream, with most points concentrated in the near wall region. The probe was positioned as close to tangent to the airfoil surface as possible at each station, such that the probe body extended downstream of the sensor and the direction of the traverse was within 5° of normal to the surface. In most cases the closest point to the wall in each profile was within about 0.2 mm of the wall, which compares to boundary layer thicknesses ranging from 1.1 mm to over 40 mm.

Flow direction in a separation bubble cannot be determined with a single-sensor hot-wire, but velocity magnitude can be measured and was found to be near zero within the bubbles of the present cases when the flow was laminar. In cases where the flow became turbulent but remained separated, fluctuating velocities caused false high mean velocity readings in the separation bubble. With the exception of these turbulent separated cases, the uncertainty in the mean velocity is 3-5%

except in the very near wall region, where near-wall corrections (Wills [43]) were applied to the mean velocity.

Velocity was also measured downstream of the cascade along the same line used for the total pressure loss measurements. Downstream and boundary layer velocity data were both time averaged and ensemble averaged based on the phase within the wake passing period. Phase averages of mean and fluctuating velocity are shown below at 24 dimensionless times, t/T, within the wake passing period, where t is time and T is the period between wakes. With the wake passing frequency of F=0.14 (corresponding to 3 Hz at Re=25,000 and 6 Hz at Re=50,000) and a 26 s data acquisition length at each measurement location, 78 and 157 wake passing periods are averaged for each ensemble for the Re=25,000 and 50,000 cases respectively.

Data were acquired at nominal Re=25,000 and 50,000. The Reynolds number, as defined above, is based on the suction surface length and the nominal cascade exit velocity. The corresponding Reynolds numbers based on the cascade inlet velocity and the axial chord length are 10,000 and 20,000. For Re=25,000, data were acquired for timings (a) and (c-i). For Re=50,000, timings (a-f) were used. Data were acquired for cases with both high and low freestream turbulence.

RESULTS

Re=25,000

The Cp and total pressure loss profiles for cases with Re=25,000 and low TI are shown in Fig. 3. The integrated total pressure losses for all cases are shown in Fig. 4. As explained in Volino [31], the integrated loss is an average of the loss coefficient across one blade spacing centered on the blade B4 wake. The inviscid Cp profile for the L1A airfoil is shown in Fig. 3a for comparison. The low peak in Cp followed by a plateau in the case without wakes indicates separation without reattachment. Wakes alone (case (a)) do not cause much change, although there is a slight drop in Cp near the trailing edge, indicating possible reattachment for part of the wake passing cycle. Little change is observed for cases (c-f). The corresponding loss profiles in Fig. 3b show no significant change from the no-wake case for cases (a-f) indicating that neither the wakes nor VGJs are effective in controlling separation. Case (g), which has two pulses evenly spaced between wakes, has slightly more of a drop in Cp near the trailing edge, which would suggest more reattachment, but no change is observed in the loss profile. Cases (h-i) show better Cp results with three pulses. In case (h) one of the VGJ disturbances coincides with the wake disturbance, while for case (i) all three pulses lie between wakes. The loss profiles for cases (h-i) agree with the Cp results, with a noticeable drop in the loss peaks, better periodicity across the cascade, and a shift in the peaks to the right. The shift corresponds to an increase in flow turning of about 3°. For the low TI, Re=25,000 cases, the variation in the integrated loss, ψ_{int}, among cases (a)-(i) is about 0.1, which is of the order of the measurement uncertainty. Although cases (h) and (i) show some improvement over the other cases, the Cp profiles are still far from reattached flow behavior, the loss profiles are still very high, and the flow turning is still well below the design point. The results suggest only partial or intermittent reattachment in cases (h) and (i), in agreement with the velocity results shown below. The timing of the VGJ pulses does not appear to matter. Cases (g) and (h) both have two pulses between wakes, but case (h) shows better results due to an extra pulse, even though this pulse occurs during a wake. Cases (h) and (i) both have three pulses, and they have similar results, even though one of the pulses in case (h) occurs during the wake. Comparison of the present results to a high Reynolds number (Re=200,000) case from Volino

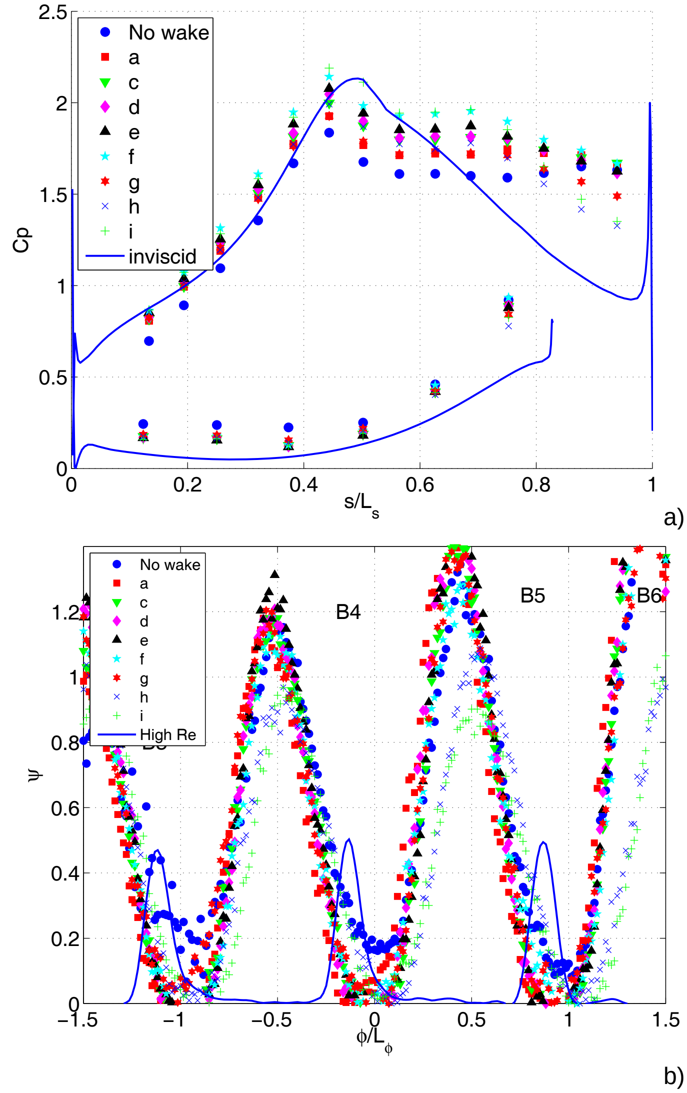

Fig. 3 Pressure profiles for low TI, Re=25,000 cases: a) Cp, b) Total pressure loss

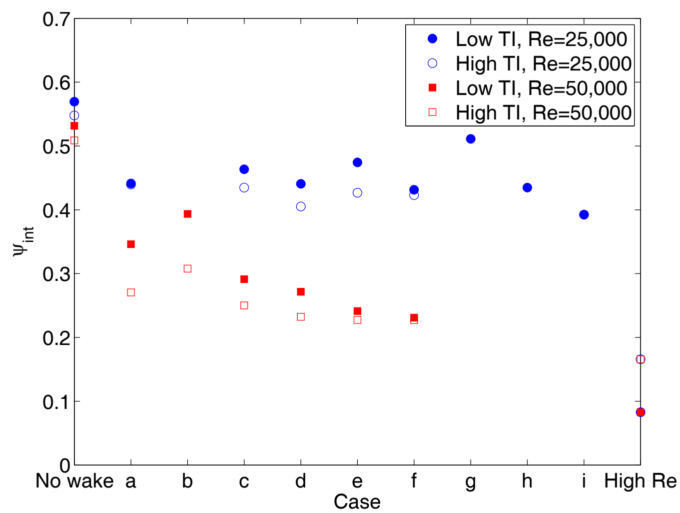

Fig. 4 Integrated total pressure loss

[31] shows that even in the best of the present cases, the loss peaks are over twice as high and there is 13° less flow turning than at high *Re*. Comparison to cases with VGJs but without wakes in Volino et al. [36] shows that loss peaks at *Re*=25,000 can be lowered another 10% and the flow turning increased another 6° if the pulsing frequency is increased to *F*=0.56. In cases (h-i) the average VGJ frequency is 0.42. The average disturbance frequency (wakes plus VGJs) in case (i) is 0.56. Comparison to cases with wakes but without VGJs in Volino [35] show similar improvements over the present results if the wake passing frequency is increased. These results suggest that the combination of wakes and VGJs is not particularly beneficial. Either can result in some separation control if the frequency is sufficiently high, but the presence of the other does not necessarily improve the results even if their combined frequency is relatively high.

Figure 5 shows the *Cp* and loss results for the high freestream turbulence *Re*=25,000 cases. Comparison of Figs. 4 and 5 shows virtually no differences. The integrated loss of Fig. 4 shows the same agreement. Boundary layer velocity results show the same similarity between the corresponding high and low *TI* cases. The same similarity between high and low *TI* is observed for all of the *Re*=50,000 cases. Previous results with wakes alone [35] or VGJs alone [36] showed that freestream turbulence effects were small compared to wake or VGJ effects on boundary layer behavior. The present results show that this small effect is reduced to near zero when both wakes and VGJs are present. Because the results for both background *TI* levels are the same, only the low *TI* results will be presented for the remainder of this paper. One result that is unexpected in Fig. 5 is the near zero loss value between wakes, as some loss should be caused by the decay of the high freestream turbulence, as seen in the high *Re* case. The near zero values may be due to bias error within the experimental uncertainty of 0.07.

Time averaged mean and fluctuating boundary layer velocity profiles are shown in Fig. 6 for the six streamwise measurements stations of Table 2. Results agree with the pressure data of Fig. 3. The separation bubble is thick for the case without wakes or VGJs. The addition of wakes (case (a)) reduces the bubble thickness only slightly. Cases (c-g) are essentially identical to each other and have a slightly thinner separation bubble than case (a). Cases (h-i), with three pulses per wake, are nearly identical to each other and show a noticeably thinner separation bubble than the other cases. It should be noted, however, that the bubble thickness is still quite thick even in cases (h-i). This agrees with the high loss and reduced flow turning compared to high *Re* results shown in Fig. 3. Comparison to cases in Volino and Ibrahim [38] shows that a reduced bubble thickness is possible if the VGJ pulsing frequency is increased to 0.56.

Figure 7 shows phase averaged mean velocity for cases (a), (c), and (d). The six columns correspond to the six streamwise stations, and the rows correspond to a few representative phases in the wake passing cycle. When the separation bubble is most distinct, the measured near wall velocity is low and nearly constant, but non-zero due to the inability of a single sensor hot-wire probe to distinguish direction in a reversing flow. When the boundary layer begins to reattach, the velocity profile goes more continuously toward zero at the wall. Cases (c) and (d) have a single VGJ pulse, and separation control is limited. Differences between the three cases in Fig. 7 are slight, but discernable. The boundary layer separates at Station 2 in all three cases, and the separation bubble grows at Station 3. The profiles for the three cases are nearly identical at Station 2. At Stations 4-6, the wake is causing some reattachment at *t/T*=0-0.333, and the profiles for the three cases are in close agreement with each other. At *t/T*=0.5-0.583, case (d) shows slight signs of reattachment at the downstream stations due to a VGJ pulse, while the other cases are more separated.

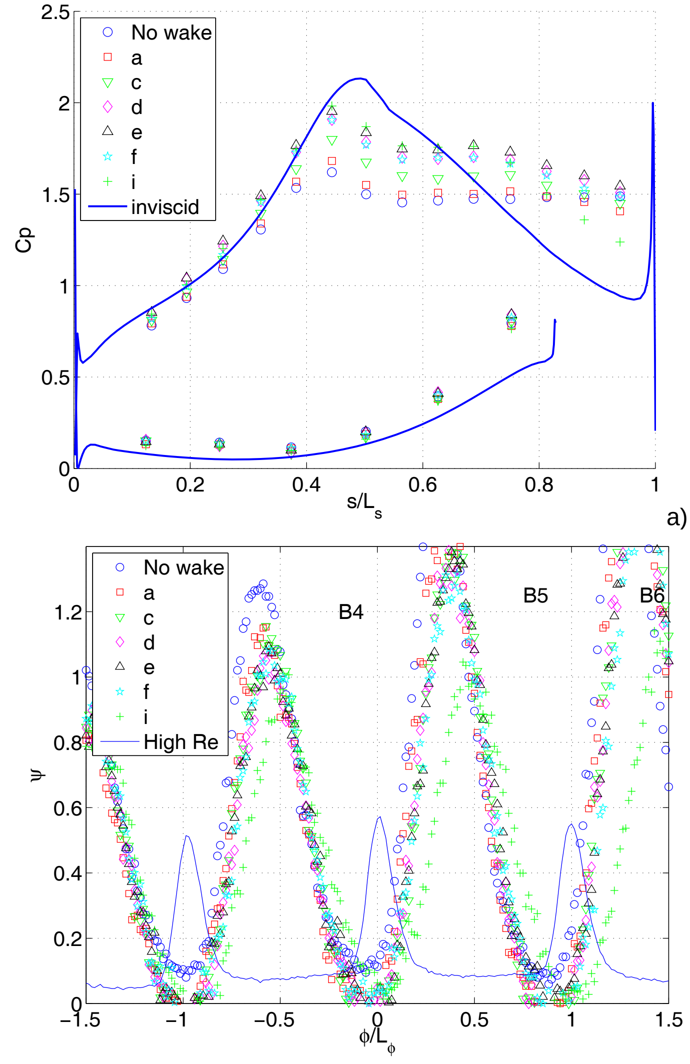

Fig. 5 Pressure profiles for high TI, Re=25,000 cases: a) Cp, b) Total pressure loss

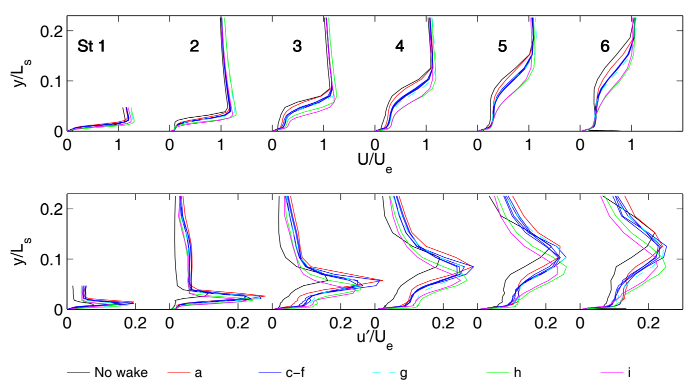

Fig. 6 Time averaged velocity profiles at six streamwise stations for low TI, Re=25,000: top – mean, bottom – rms

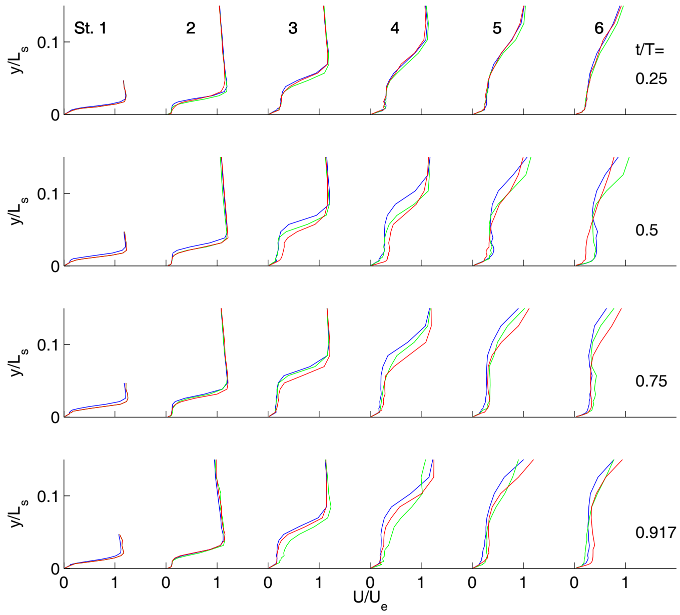

Fig. 7 Phase averaged mean velocity profiles for Re=25,000 cases, columns for six streamwise stations, rows for phases in pulsing cycle: blue – case (a), green – case (c), red – case (d)

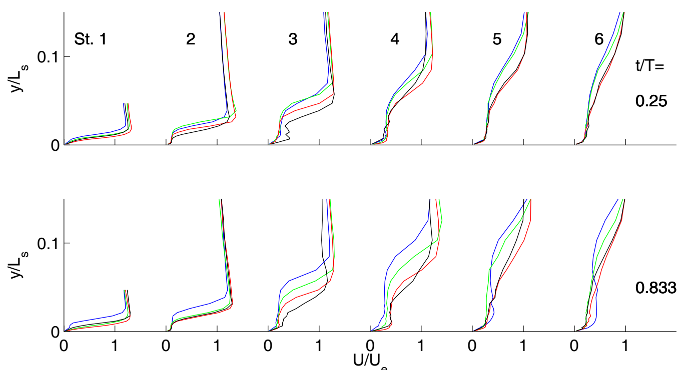

Fig. 8 Phase averaged mean velocity profiles for Re=25,000 cases: blue – case (a), green – case (g), red – case (h), black – case (i)

At t/T=0.667-0.75 all cases show a thick separation bubble. At t/T=0.833, case (c) shows reattachment at Station 3 due to a VGJ pulse, and this continues to Station 4 at t/T=0.917 and Station 5 at t/T=1. The profiles of Fig. 7 show that the VGJ pulses clearly do have some effect, albeit small at this *Re*, and the appearance of the effect depends on the jet timing, although overall separation control is very limited, as shown by the time averaged profiles of Fig. 6.

Figure 8 shows the effect of multiple VGJ pulses on the phase averaged velocity. Case (a), shown for reference, has only wakes. Case (g) has two pulses between the wakes. Case (h) has three pulses, with two occurring at about the same timings as in case (g) and the third coinciding with the wake. Case (i) has three pulses between wakes. Comparison to Fig. 7 shows that separation control is better with multiple jet pulses, in agreement with the time averaged profiles of Fig. 6. Cases (a) and (g) are in close agreement for t/T=0-0.333, which corresponds to the wake passing. At later times, case (g) shows a somewhat thinner separation bubble than case (a) as the VGJs help to control separation. With some minor exceptions, cases (h) and (i) are in good agreement with each other for the full cycle. The addition of a third VGJ pulse reduces separation from case (g) at all phases, both during and between wakes. Whether the third pulse occurs during or between wakes does not seem to matter. With three pulses the separation bubble is present at Stations 2-4, but by the downstream stations the VGJ pulses occur frequently enough to prevent a distinct bubble from forming. The strong adverse pressure gradient still results in a thick boundary layer in cases (h-i), and at some phases the boundary layer is on the verge of separating.

The time averaged boundary layer thickness, $\delta_{99.5}$, is shown in Fig. 9 for the *Re*=25,000 cases, and these values are used in Fig. 10, which shows the phase averaged separation bubble thickness as a fraction of the local, time averaged $\delta_{99.5}$. The bubble thickness is estimated as the distance from the wall to the farthest point in the shear layer with $\partial u / \partial y$ <0. The bubble thickness as a fraction of the boundary layer thickness is used to show the local extent of separation. One could also use the shape factor, but the uncertainty in the displacement and momentum thicknesses resulting from the inability of the hot wire to accurately measure velocity within the separation bubble makes the shape factor a somewhat less reliable quantity than the bubble thickness used here. The dimensional bubble thickness at any given time and location can be determined using the data in Figs. 9 and 10 together. In each time-space plot of Fig. 10, the data are repeated for two cycles to show the periodicity. The solid and dashed white lines indicate the leading and trailing edges of the wake affected regions. The magenta lines bound the VGJ affected regions. In all cases, the suppression of the bubble by both the wake and VGJs is clear. As shown in previous studies ([4], [38], [37]), the initial transient at the start of a VGJ pulse is most effective for flow control. For the wakes, it appears that the separation control is effective for the full duration of the wake. Hence, the separation bubble is suppressed for about three times as long by each wake than by each VGJ pulse. Cases (g) and (h) appear very similar in Fig. 10, which would suggest that the extra pulse within the wake of case (h) is ineffective. The normalizing quantity, $\delta_{99.5}$ is lower for case (h), however, so the extra pulse does help, as shown in Figs. 3, 6 and 8.

The effects of the boundary layer behavior on the downstream flow are shown in Figs. 11 and 12, which show the phase averaged mean and fluctuating velocity $0.63C_x$ downstream of the blade row. The phase averaged mean velocity is the average of all the velocity data at a particular location and phase. The fluctuating velocity is the rms of the difference between the instantaneous velocity and the local phase averaged mean at each location and phase. Cases (a) and (i) are shown as examples. The contours are normalized by the exit velocity U_e. Since the rod spacing is $2L_\phi$, the flow in alternating passages is in phase, with the passages between a half cycle out of phase. In Figs. 11a and 12a, there are vertical strips of low mean velocity at ϕ/L_ϕ = -1.5, -0.5, 0.5 and 1.5 which result from the velocity deficit in the airfoil wakes. Strips of high fluctuating velocity are present at these same locations in Figs. 11b and 12b. These positions correspond to the loss peaks in Fig. 3b. The dimensionless mean velocity between the airfoil wakes cycles between a low of about 0.85 and a high of about 1.1 showing the velocity deficit in the rod wakes and the acceleration between wakes. The rod wakes proceed at an angle in the figure, rising from left to right, as they move forward in time and transit across the cascade. The highest turbulence peaks occur where the rod wakes interact with the separation bubble and airfoil wakes. Comparing Figs. 11 and 12, the amount of mean velocity variation and turbulence in case (i) is less than in case (a) as the VGJs reduce the amount of separation and reattachment in the boundary layer. The separation control, as shown above, is not complete, however, so the

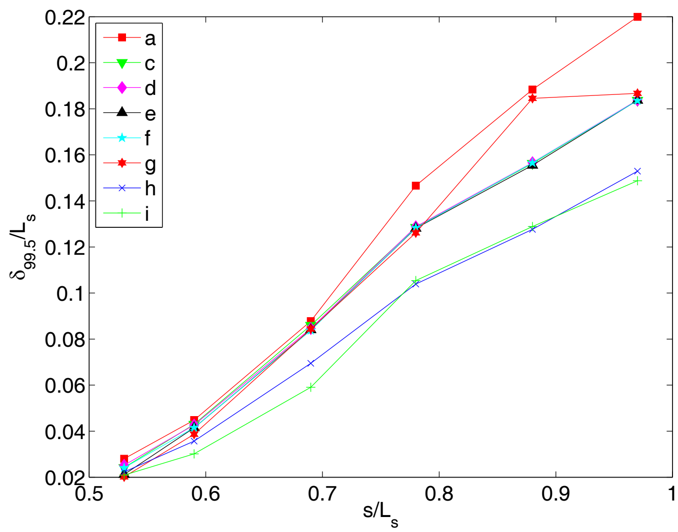

Fig. 9 Time averaged boundary layer thickness, $\delta_{99.5}$, for Re=25,000 cases

results for case (a) with wakes only and case (i) with the best control of the cases considered at *Re*=25,000, are not drastically different. Larger differences were observed in Volino [35] in cases where higher wake passing frequencies resulted in better separation control.

Re=50,000

When the Reynolds number is increased to 50,000, the boundary layer is less prone to separation and more easily controlled. As noted above, full data sets were acquired at *Re*=50,000 for both high and low background freestream turbulence, but since the high and low *TI* results are nearly indistinguishable, only the low *TI* results are presented below. The *Cp* and total pressure loss profiles are shown in Fig. 13. Without wakes or VGJs, the boundary layer separates and does not reattach. With wakes alone (case (a)) the *Cp* profile shows a large drop near the trailing edge, indicating reattachment, but the peak *Cp* value is below the value in the better controlled cases, indicating that reattachment is likely not complete for the full cycle. Cases (b), which has a single VGJ pulse occurring coincident with the wake, matches case (a), indicating that the single pulse provides no benefit when it overlaps the wake. In cases (c) and (d), which both have a single VGJ pulse between wakes, the separation control is better. The *Cp* profiles suggest a bubble is present between s/L_s=0.6 and 0.8, but the boundary layer is attached farther downstream. With two pulses per wake in cases (e) and (f), results are similar, but reattachment appears to move slightly upstream. The loss profiles of Fig. 12b are consistent with the *Cp* results, particularly for the center blade, B4. Cases (a) and (b) are similar to each other and have loss peaks about 30% lower than in the case without wakes. This is consistent with the integrated results shown in Fig. 4. The peaks are also shifted to the right of the no-wake case, indicating an increase in flow turning of about 3°. For cases (c-f) there is an additional drop in the loss peak and a further shift to the right, indicating about 8° more flow turning than the no-wake case. Even in the best case the loss peak is much larger and indicates about 5° less flow turning than in the high Reynolds number comparison case. For cases (e) and (f), which have the best separation control, the wakes of blades B4 and B5 appear similar. For the other cases, the control is partial and as noted above the tailboard has an effect of further suppressing separation on the closer blades, resulting in poorer periodicity. This effect may be more apparent at *Re*=50,000 than in the *Re*=25,000 case of Figs. 3 and 5

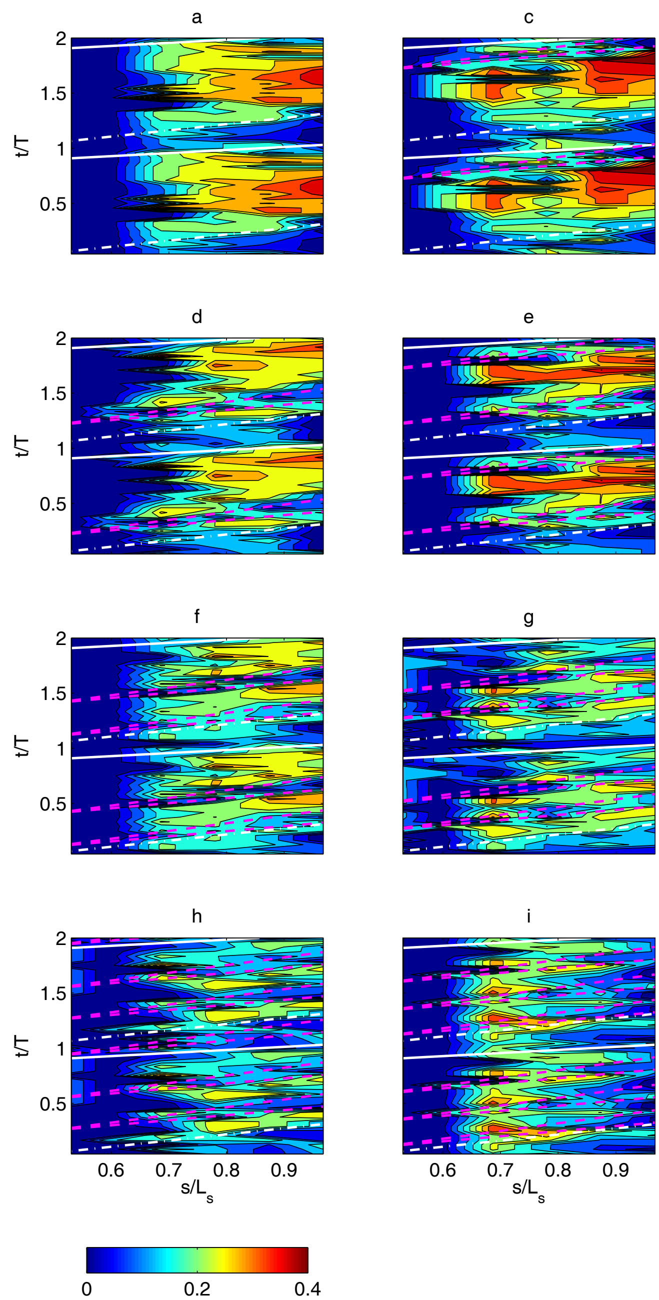

Fig. 10 Time space plots of phase averaged separation bubble thickness normalized on local time averaged $\delta_{99.5}$ for Re=25,000 cases: solid white line – leading edge of wake, dashed white line – trailing edge of wake, magenta lines – extent of VGJ affected region

since *Re*=50,000 is a borderline case with respect to separation, and the boundary layer can go from fully separated to nearly fully attached with relatively small changes in conditions. This appears to make the boundary layer more sensitive to the influence of the tailboard and leads to differences between passages. At Re=25,000, separation control was only partial even in the best cases. The tailboard may act to reduce the bubble thickness more in some passages than others, but it is less likely to produce reattachment. Hence there tends to be more variability between passages at Re=50,000 than 25,000.

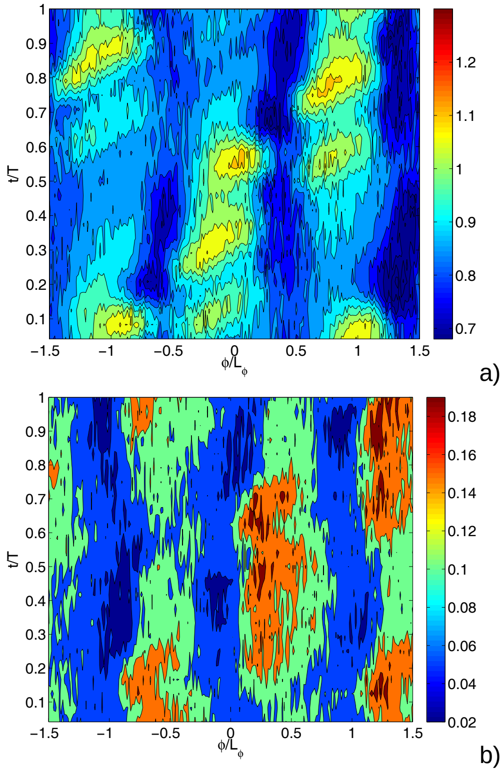

Fig. 11 Time space plot of phase averaged velocity 0.63C$_x$ downstream of cascade for Re=25,000 case (a): a) U/U$_e$, b) u′/U$_e$

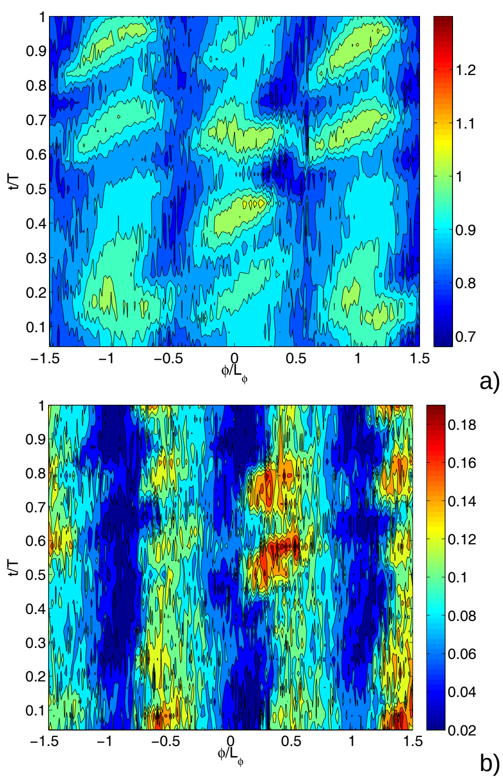

Fig. 12 Time space plot of phase averaged velocity 0.63C$_x$ downstream of cascade for Re=25,000 case (i): a) U/U$_e$, b) u′/U$_e$

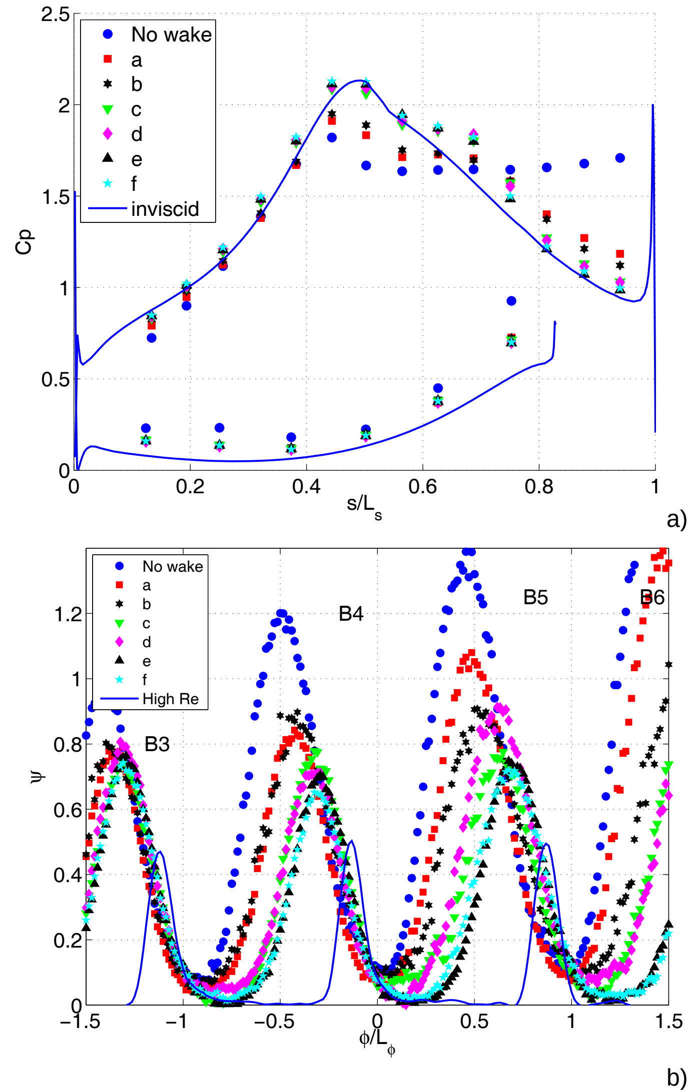

Fig. 13 Pressure profiles for low TI, Re=50,000 cases: a) Cp, b) Total pressure loss

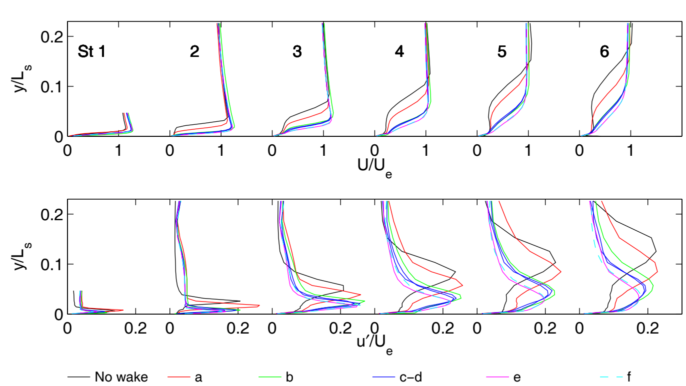

Fig. 14 Time averaged velocity profiles at six streamwise stations for low TI, Re=50,000: top – mean, bottom – rms

Time averaged velocity profiles for the Re=50,000 cases are shown in Fig. 14. Without wakes there is a large separation bubble, in agreement with the pressure results of Fig. 13. With wakes alone in case (a), the separation bubble is slightly thinner. In cases (b-d), which all have one VGJ pulse per wake, the separation bubble is much thinner. At Station 6, there is no clear separation bubble, although the boundary layer appears to be on the verge of separating. In the mean profiles, cases (b-d) are virtually indistinguishable from each other. In the fluctuating profiles, the peak in case (b) is slightly farther from the wall than in cases (c-d). This result agrees with the trend in Fig. 13, which shows that separation control is slightly less effective when the pulse coincides with the wake, but the differences associated with the timing are small and are not apparent in all measured quantities. In cases (e-f), which have two pulses per wake, the separation bubble is slightly thinner than in cases (b-d), and the peak in the fluctuating velocity is smaller and closer to the wall.

The boundary layer thicknesses, determined from the profiles of Fig. 14, are shown in Fig. 15. Figure 16 shows the phase averaged separation bubble thickness as a fraction of $\delta_{99.5}$. The wake and VGJ pulses both suppress separation at all locations. Between wakes and pulses the boundary layer separates at s/L_s≈0.7 in all cases. Without VGJs (case (a)) this separation persists to the trailing edge. With VGJs, regardless of timing, the boundary layer reattaches at all phases.

Figures 17 and 18 show the phase averaged mean and fluctuating velocity in the airfoil wakes for cases (a) and (e). As in Figs. 11 and 12, the velocity deficits and turbulence in the airfoil wakes are clear at ϕ/L_ϕ = -1.5, -0.5, 0.5 and 1.5. The rod wakes appear between the airfoil wakes as areas of slightly elevated fluctuating velocity in Figs. 16b and 17b at ϕ/L_ϕ = -1, and 1 when t/T=0.15; and at ϕ/L_ϕ = 0 when t/T=0.65. As in Figs. 11 and 12, the fluctuating velocity is highest when the rod wakes interact with the airfoil wakes. The variation in the mean velocity and the turbulence are lower for case (e) than case (a) because the VGJs reduce the growth of the separation bubble. The reduction in wake strength and turbulence is in agreement with the thinner boundary layer and separation bubble shown in Figs. 14-16, and the reduced losses of Fig. 13b. Wake measurements for the other Re=50,000 cases show the same trend.

The results at both Re=25,000 and 50,000 show that when acting together, wakes and VGJs suppress separation. This result is expected since wakes and VGJs were both previously shown to suppress separation when acting alone. Somewhat surprisingly, the boundary layer was not very sensitive to the timing of the VGJs with respect to the wakes. It had been expected that VGJs timed to pulse between wakes would help suppress the growth of the separation bubble between the wakes, while VGJs timed to coincide with the wakes might be wasted since the wake would already be acting to suppress separation at the instant when the jets were pulsed. Cases (b-d) at Re=50,000 indicate that timing the VGJs to avoid the wakes may have some benefit, but the influence of timing is small. A pulse lying completely within a wake (case (b)) still helps suppress separation and reduce losses, and is nearly as effective as a pulse between wakes (cases (c) and (d)). For the Re=25,000 cases, two pulses between wakes (case (g)) were not enough to significantly reduce separation and losses, but when a third pulse was added within the wake (case (h)), separation was reduced. In fact, case (h) was just as effective as case (i), which had all three pulses between wakes.

CONCLUSIONS

The combined effects of unsteady wakes and vortex generator jets on the flow over the very high lift L1A airfoil were studied experimentally under low and high freestream turbulence conditions.

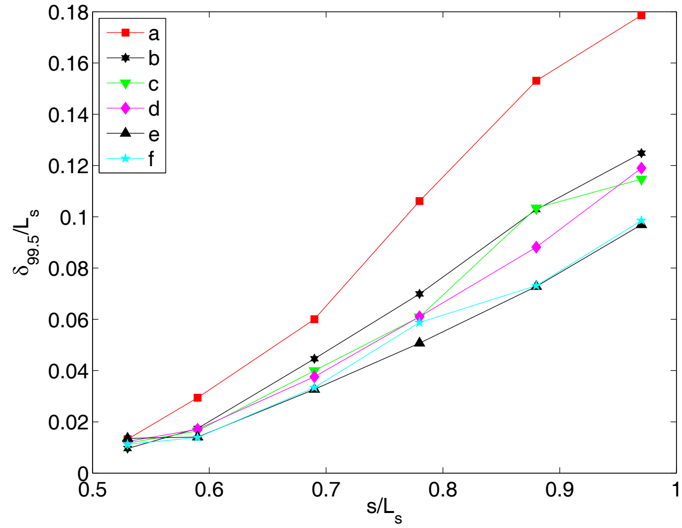

Fig. 15 Time averaged boundary layer thickness, $\delta_{99.5}$, for Re=50,000 cases

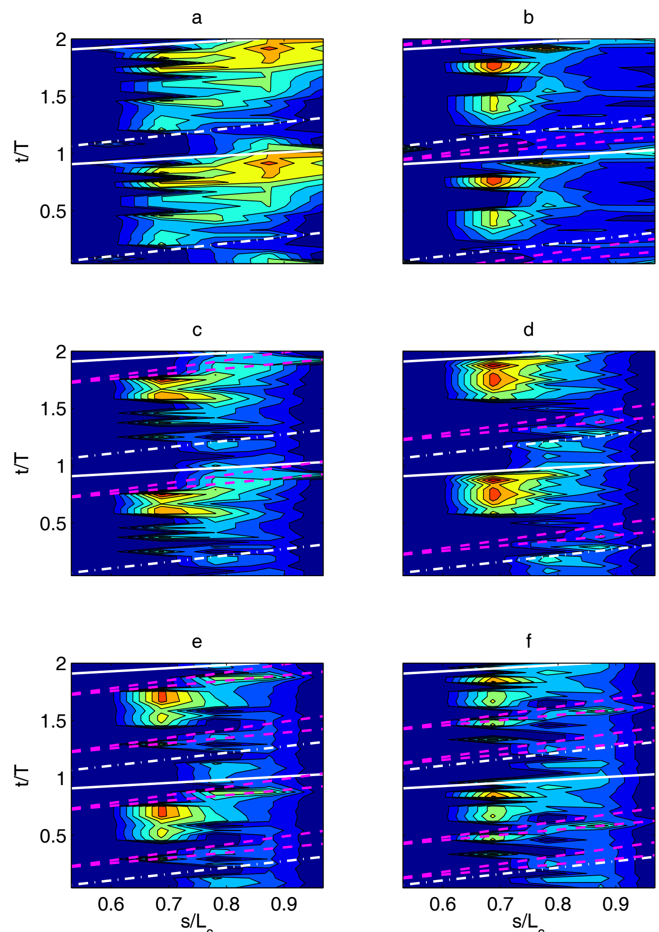

Fig. 16 Time space plots of phase averaged separation bubble thickness normalized on local time averaged $\delta_{99.5}$ for Re=50,000 cases: solid white line – leading edge of wake, dashed white line – trailing edge of wake, magenta lines – extent of VGJ affected region (same color scale as Fig. 9)

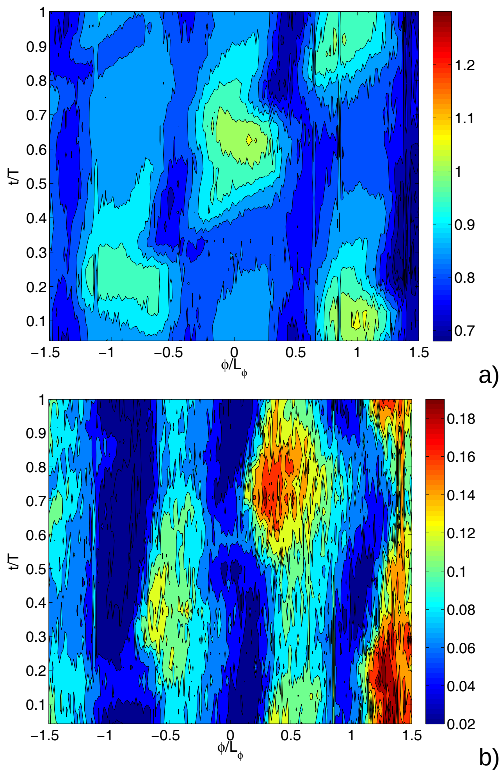

Fig. 17 Time space plot of phase averaged velocity 0.63C_x downstream of cascade for Re=50,000 case (a): a) U/U_e, b) u'/U_e

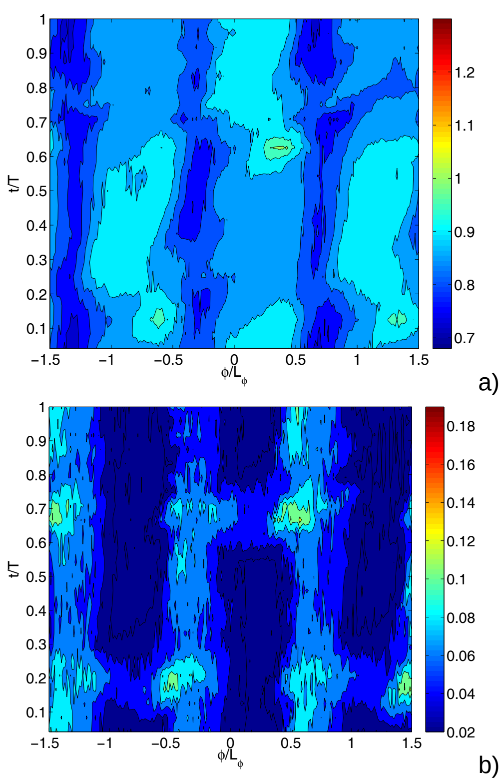

Fig. 18 Time space plot of phase averaged velocity 0.63C_x downstream of cascade for Re=50,000 case (e): a) U/U_e, b) u'/U_e

Reynolds numbers based on suction surface length and nominal exit velocity of 25,000 and 50,000 were considered. The effect of the background freestream turbulence between wakes was negligible in the presence of larger wake and VGJ disturbances. Results for cases with *TI*=0.6% and 4% were nearly identical. The wake passing frequency considered in the present study was sufficiently low that the wakes caused only intermittent reattachment with a large, unclosed separation bubble appearing between wakes. Vortex generator jets were able to help reduce this separation if their pulsing frequency was sufficiently high. The timing of the jets with respect to the wakes was not particularly important. For the cases considered, the beneficial effects of the wakes and VGJs did not appear to be additive. The jet pulsing frequency required to fully control separation was about the same as needed in cases without wakes.

ACKNOWLEDGMENTS

This work was sponsored by the National Aeronautics and Space Administration under grant NNC07IA10I. The grant monitors were Drs. Anthony Strazisar and James Heidmann of the NASA Glenn Research Center. The support of the United States Naval Academy Technical Support Department Shop and Fluids Laboratory is greatly appreciated.

REFERENCES

[1] Hourmouziadis, J., 1989, "Aerodynamic Design of Low Pressure Turbines," AGARD Lecture Series 167.

[2] Mayle, R.E., 1991, "The Role of Laminar-Turbulent Transition in Gas Turbine Engines," ASME *Journal of Turbomachinery*, **113**, pp. 509-537.

[3] Sharma, O.P., Ni, R.H., and Tanrikut, S., 1994, "Unsteady Flow in Turbines," AGARD Lecture Series 195, Paper No. 5.

[4] Bons, J.P., Sondergaard, R., and Rivir, R.B., 2001, "Turbine Separation Control Using Pulsed Vortex Generator Jets," ASME *Journal of Turbomachinery*, **123**, pp. 198-206.

[5] Volino, R.J., and Hultgren, L.S., 2001, "Measurements in Separated and Transitional Boundary Layers Under Low-Pressure Turbine Airfoil Conditions," ASME *Journal of Turbomachinery*, **123**, pp. 189-197.

[6] Hodson, H.P., and Howell, R.J., 2005, "Bladerow Interactions, Transition, and High-Lift Aerofoils in Low-Pressure Turbine," *Annual Review of Fluid Mechanics*, **37**, pp. 71-98.

[7] Gostelow, J.P., Walker, G.J., Solomon, W.J., Hong, G., and Melwani, N., 1997, "Investigation of the Calmed Region Behind a Turbulent Spot," ASME *Journal of Turbomachinery*, **119**, pp. 802-809.

[8] Schulte, V., and Hodson, H.P., 1998, "Prediction of the Becalmed Region for LP Turbine Profile Design," ASME *Journal of Turbomachinery*, **120**, pp. 839-846.

[9] Bons, J.P., Pluim, J., Gompertz, K., Bloxham, M., and Clark, J.P., 2008, "The Application of Flow Control to an Aft-Loaded Low Pressure Turbine Cascade with Unsteady Wakes," ASME Paper GT2008-50864.

[10] Pluim, J., Memory, C., Bons, J., and Chen, J.P., 2009, "Designing a High Fidelity Wake Simulator for Research Using Linear Cascades," ASME Paper GT2009-52276.

[11] Schobeiri, M.T., Öztürk, B., and Ashpis, D.E., 2007, "Effects of Reynolds Number and Periodic Unsteady Wake Flow Condition on Boundary Layer Development, Separation, and Intermittency Behavior Along the Suction Surface of a Low Pressure Turbine Blade," ASME *Journal of Turbomachinery*, **129**, pp. 92-107.

[12] Öztürk, B., and Schobeiri, M.T., 2007, "Effects of Turbulence Intensity and Periodic Unsteady Wake Flow Condition on Boundary Layer Development, Separation, and Reattachment Along the Suction Surface of a Low-Pressure Turbine Blade," ASME *Journal of Fluid Engineering*, **129**, pp. 747-763.

[13] Jiang, N., and Simon, T.W., 2005, "Transition in Low-Pressure Turbines: Effects of Unsteady Acceleration and Turbulence Intensity," AIAA *Journal of Thermophysics and Heat Transfer*, **19**, 148-155.

[14] Mahallati, A., and Sjolander, S.A., 2007, "Aerodyanmics of a Low-Pressure Turbine Airfoil at Low-Reynolds Numbers Part 2: Blade-Wake Interaction," ASME Paper GT2007-27348.

[15] Zhang, X.F., and Hodson, H.P., 2010, "Effects of Reynolds Number and Freestream Turbulence Intensity on the Unsteady Boundary Layer Development on an Ultra-High-Lift Low Pressure Turbine Airfoil," ASME *Journal of Turbomachinery*, **132**, 011016.

[16] Funazaki, K., Yamada, K., Ono, T., Segawa, K., Hamazaki, H., Takahashi, A., and Tanimitsu, H., 2006, "Experimental and Numerical Investigations of Wake Passing Effects upon Aerodynamic Performance of a LP Turbine Linear Cascade With Variable Solidity," ASME Paper GT2006-90507.

[17] Praisner, T.J., and Clark, J.P., 2007, "Predicting Transition in Turbomachinery – Part 1: A Review and New Model Development," ASME *Journal of Turbomachinery*, **129**, pp. 1-13.

[18] Zhang, X.F., Vera, M., Hodson, H., and Harvey, N., 2007, "Separation and Transition Control on an Aft-Loaded Ultra-High-Lift LP Turbine Blade at Low Reynolds Numbers: Low-Speed Investigation," ASME *Journal of Turbomachinery*, **128**, pp. 517-527.

[19] Bohl, D.G., and Volino, R.J., 2006, "Experiments with Three-Dimensional Passive Flow Control Devices on Low-Pressure Turbine Airfoils," ASME *Journal of Turbomachinery*, **128**, pp. 251-260.

[20] Volino, R.J., 2003, "Passive Flow Control on Low-Pressure Turbine Airfoils," ASME *Journal of Turbomachinery*, **125**, pp. 754-764.

[21] Huang, J., Corke, T., and Thomas, F., 2003, "Plasma Actuators for Separation Control on Low Pressure Turbine Blades," AIAA Paper 2003-1027.

[22] Johnston, J.P., and Nishi, M., 1990, "Vortex Generator Jets. Means for Flow Separation Control," *AIAA Journal*, **28**, pp. 989-994.

[23] Bons, J.P., Sondergaard, R., and Rivir, R.B., 2002, "The Fluid Dynamics of LPT Blade Separation Control Using Pulsed Jets," ASME *Journal of Turbomachinery*, **124**, pp. 77-85.

[24] Volino, R.J., 2003, "Separation Control on Low-Pressure Turbine Airfoils Using Synthetic Vortex Generator Jets," ASME *Journal of Turbomachinery*, **125**, pp. 765-777.

[25] Volino, R.J., and Bohl, D.G., 2005, "Structure of Oscillating Vortex Generator Jets," Proceedings of the Fourth International Symposium on Turbulence and Shear Flow Phenomena, **2**, pp. 589-594.

[26] McQuilling, M., and Jacob, J., 2004, "Effect of Chord Location on Separation Control With Vortex Generator Jets on Low Pressure Turbine Blades," AIAA Paper 2004-2205.

[27] Eldredge, R. G., and Bons, J. P., 2004, "Active Control of a Separating Boundary Layer With Steady Vortex Generating Jets—Detailed Flow Measurements," AIAA Paper 2004-751.

[28] Bons, J.P., Reimann, D., and Bloxham, M., 2008, "Separated Flow Transition on an LP Turbine Blade With Pulsed Flow Control," ASME *Journal of Turbomachinery*, **130**, 021014.

[29] Clark J.P., 2007, Private Communication, Air Force Research Laboratory.

[30] Zhang, X.F., and Hodson, H., 2005, "Combined Effects of Surface Trips and Unsteady Wakes on the Boundary Layer Development of an Ultra-High-Lift LP Turbine Blade," ASME *Journal of Turbomachinery*, **127**, pp. 479-488.

[31] Volino, R.J., 2010, "Separated Flow Measurements on a Highly Loaded Low-Pressure Turbine Airfoil," ASME *Journal of Turbomachinery*, **132**, 011007.

[32] Ibrahim, M., Kartuzova, O., and Volino, R.J., 2008, "Experimental and Computational Investigations of Separation and Transition on a Highly Loaded Low Pressure Turbine Airfoil: Part 1 – Low Freestream Turbulence Intensity," ASME Paper IMECE2008-68879.

[33] Volino, R.J, Kartuzova, O., and Ibrahim, M., 2008, "Experimental and Computational Investigations of Separation and Transition on a Highly Loaded Low Pressure Turbine Airfoil: Part 2 – High Freestream Turbulence Intensity," ASME Paper IMECE2008-68776.

[34] Volino, R.J., 2002, "Separated Flow Transition Under Simulated Low-Pressure Turbine Airfoil Conditions: Part 1 – Mean Flow and Turbulence Statistics," ASME *Journal of Turbomachinery*, **124**, pp. 645-655.

[35] Volino, R.J., 2010, "Effect of Unsteady Wakes on Boundary Layer Separation on a Very High Lift Low Pressure Turbine Airfoil," ASME Paper GT2010-23573.

[36] Volino, R.J., Kartuzova, O., and Ibrahim, M.B., 2009, "Experimental and Computational Investigations of Low-Pressure Turbine Separation Control Using Vortex Generator Jets," ASME Paper GT2009-59983.

[37] Volino, R.J., Kartuzova, O., and Ibrahim, M.B., 2010, "Separation Control on a Very High Lift Low Pressure Turbine Airfoil Using Pulsed Vortex Generator Jets," ASME Paper GT2010-23567.

[38] Volino, R.J., and Ibrahim, M.B., 2010, "Separation Control on High Lift Low Pressure Turbine Airfoils Using Pulsed Jet Vortex Generator Jets," Proceedings of the ASME-ATI-UIT 2010 Conference on Thermal and Environmental Issues in Energy Systems, 2010.

[39] Ibrahim, M., Kartuzova, O., Doucet, D., and Volino, R.J., 2010, "LES Flow Control Simulations for Highly Loaded Low Pressure Turbine Airfoil (L1A) Using Pulsed Vortex Generator Jets," ASME paper GT2010-23015.

[40] Ibrahim, M.B., Kartuzova, O., and Volino, R.J., 2009, "LES and URANS Computational Investigations of LPT Blade (L1A) Separation Control using Vortex Generator Jets," Proceedings of Turbulence, Heat and Mass Transfer 6, 2009.

[41] Bloxham, M., Reimann, D., Crapo, K., Pluim, J., and Bons, J.P., 2007, "Synchronizing Separation Flow Control with Unsteady Wakes in a Low-Pressure Turbine Cascade," ASME Paper GT2007-27529.

[42] Kaszeta, R.W., Simon, T.W., Jiang, N., and Ottaviani, F., 2005, "Influence of Wake Passing Frequency and Elevated Turbulence Intensity on Transition," AIAA *Journal of Thermophysics and Heat Transfer*, **19**, 137-147.

[43] Wills, J.A.B., 1962, "The Correction of Hot-Wire Readings for Proximity to a Solid Boundary," *Journal of Fluid Mechanics*, **12**, pp. 65-92.